RSC Advances

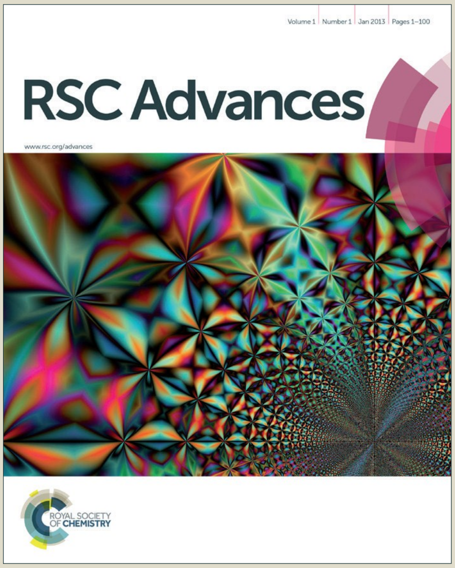

ROYAL SOCIETY OF CHEMISTRY

www.rsc.org/advances

RSC Advances

Photoreduction of CO_2 to CO by a mononuclear Re(I) complex and DFT evaluation of the photocatalytic mechanism

Jamaladin Shakeri,[a,b] Hossein Farrokhpour,*[a] Hassan Hadadzadeh,*[a] and
Mohammad Joshaghani [b]

[a] Department of Chemistry, Isfahan University of Technology, Isfahan 84156-83111, Iran
[b] Faculty of Chemistry, Razi University, Kermanshah, 67149, Iran

Number of Pages: 32
Number of Schemes: 6
Number of Tables: 2
Number of Figures: 6

***Corresponding authors:**

Hossein Farrokhpour,

Assistant Professor of Physical Chemistry

Department of Chemistry, Isfahan University of Technology, Isfahan 84156-83111, Iran

E-mail address: h-farrokh@cc.iut.ac.ir

Hassan Hadadzadeh,

Professor of Inorganic Chemistry

Department of Chemistry, Isfahan University of Technology, Isfahan 84156-83111, Iran

E-mail address: hadad@cc.iut.ac.ir

RSC Advances

Photoreduction of CO_2 to CO by a mononuclear Re(I) complex and DFT evaluation of the photocatalytic mechanism

Jamaladin Shakeri,[a,b] Hossein Farrokhpour,*[a] Hassan Hadadzadeh,*[a] and Mohammad Joshaghani [b]

[a] Department of Chemistry, Isfahan University of Technology, Isfahan 84156-83111, Iran

[b] Faculty of Chemistry, Razi University, Kermanshah, 67149, Iran

Abstract

A new method was reported for the high-yield synthesis of a mononuclear Re(I) complex, *fac*-[Re(phen-dione)$(CO)_3$Cl] (where phen-dione = 1,10-phenanthroline-5,6-dione). The photochemical activity of the Re(I) complex for the photoreduction of CO_2 to CO was investigated under different conditions. The density functional theory (DFT) calculations were used to evaluate the photocatalytic mechanism for the photoreduction of CO_2 to CO in the presence of the Re(I) complex as a photocatalyst through a detailed comparison of two potential pathways: (I) regeneration of the initial catalyst, and (II) formation of a solvent–coordinated Re(I) complex. Although the theoretical calculations reveal that the regeneration of the initial photocatalyst through the reassociation of the Re(I) cationic intermediate with Cl^- is more thermodynamically favorable than the formation of a solvent–coordinated Re(I) species, the present results show that the both catalytic cycles with inclusion of solvation effect are thermodynamically favorable.

---

*Corresponding authors. Tel.: +98 3133913240; fax: +98 3133912350.

E-mail addresses: h-farrokh@cc.iut.ac.ir (H. Farrokhpour), and hadad@cc.iut.ac.ir (H. Hadadzadeh).

Introduction

CO_2 is one of several polyatomic molecules that are implicated in the greenhouse effect. Its increase in the atmosphere is considered as a major contributor to global warming and the climate changes that come as a direct consequence.[1] Carbon has three main oxides, CO, CO_2, and C_3O_2 (carbon suboxide or tricarbon dioxide). CO_2 is the most thermodynamically stable oxide of carbon at room temperature which requires a lot of energy to convert into other chemicals.[2] In recent years, the chemical conversion of CO_2 into useful chemicals such as CO (as a fuel: $CO + 1/2\ O_2 \rightarrow CO_2 + \text{Energy}$) is an interesting solution to the world's demand for fuels, decrease of greenhouse gas emissions, and recycling of carbon (Scheme 1).[3] Particularly, the use of mononuclear tricarbonyl polypyridyl rhenium(I) complexes such as $[Re(diimine)(CO)_3X]$ (X = Cl^-, Br^-, CN^-, and SCN^-; and diimine = bpy, phen, phen-dione, and dppz) for reduction of CO_2 have attracted a lot of attention due to their ability to absorb light, store redox equivalents, and convert CO_2 into higher-energy products.[4-10] These complexes, with various X, exhibit different catalytic activities while keeping aromatic diimine ligands constant. For example, in *fac*-$[Re(bpy)(CO)_3X]$ (X = SCN^-, Cl^-, and CN^-) complexes, it has been identified that the photocatalytic activities of these three complexes for reduction of CO_2 to CO are very different. In the case of X = SCN^-, 60 μmol of CO gas was produced after 25 h of irradiation, which was two times higher than the value found in X = Cl^- under the same condition; although, X = CN^- cannot act as a photocatalyst.[7] Also, rhenium complexes with different aromatic diimine ligands and appropriate X ligand have been the subject of several studies.[8] For example, Kubiak and co-workers [9,10] have reported the improved electrocatalytic activity by altering the substituent at the 4- and 4′- positions of the bipyridine (bpy) ligand. The complex with 4,4′-*t*Bu_2bpy exhibits a catalytic activity for reduction of CO_2 which is about four times greater than that is observed with a simple bipyridine complex.

One interesting feature of CO_2 reduction by Re complexes is investigation of the photocatalytic and electrocatalytic mechanisms involved in this reduction.[11] In particular, the mechanism of the photochemical reduction of CO_2 by rhenium complexes has been largely studied so far. In General, due to the presence of different species in solution, an exact determination of the photocatalytic mechanism in solution is often difficult. Some of these species are as follows: triethylamine (TEA) or triethanolamine (TEOA) as the sacrificial electron donor, the solvent that has ability to coordinate to metal ions (dimethylformamide (DMF), dimethyl sulfoxide (DMSO), or CH_3CN), the subsequent byproducts, different intermediates, and sometimes NR_4Cl (R = Et or Bu) as a chloride source. Upon irradiation, the Re(I) complex is promoted to an MLCT excited state with a Re(II) metal center and an electron located on the empty π^* orbital of polypyridyl ligands. Sacrificial electron donors are added in excess to quench the excited state and prevent the back-electron transfer. In this step, a one-electron-reduced (OER) intermediate is formed, which is an initiator for photocatalytic reaction. After the dissociation of chloride anion, a solvent-coordinated Re(I) complex is formed. The CO_2-coordinated rhenium complex is one of the most important intermediates in the photocatalytic reduction of CO_2 to CO, which has been previously investigated for $[Re(dmbpy)(CO)_3Cl]$.[12] For the first time, a CO_2-coordinated rhenium bipyridyl complex, $[Re(dmbpy)(CO)_3(COOH)]$, has been successfully detected by cold-spray ionization mass spectrometry (CSI-MS).[12] On the basis of previous experimentally studies, the photocatalytic mechanism for the reduction of CO_2 to CO in the presence of the Re(I) complex as a photocatalyst has been also investigated through a detailed comparison of two potential pathways: (**I**) regeneration of the initial catalyst through the reassociation of the Re(I) cationic intermediate with Cl^-, investigated by Ishitani and co-workers;[7] and (**II**) formation of a solvent–coordinated Re(I) complex without the replacement of Cl^-, proposed by Inoue's group.[12] Although, much research has been done on the mechanism of the photochemical reduction of CO_2 by rhenium complexes, but there are still some questions left unanswered about the intermediates and the reaction pathways.

In this study, a new method for the preparation of a mononuclear Re(I) phen-dione complex, *fac*-[Re(phen-dione)$(CO)_3$Cl], and its photocatalytic activity for reduction of CO_2 to CO have been reported. In addition, the theoretical calculations, at the density functional theory (DFT), were used to evaluate the photocatalytic mechanism for the photoreduction of CO_2 to CO. The free energy profiles of the considered mechanisms were also obtained and discussed. Two mechanisms have been proposed for the photocatalytic reduction of CO_2 to CO using this mononuclear Re(I) complex.

2. Experimental

2.1. Materials and measurements

All chemicals and solvents were commercially available in high purity and used without further purification. $Re_2(CO)_{10}$ (dirhenium decacarbonyl) was purchased from Merck. 1,10-phenanthroline-5,6-dione (phen-dione), 2-chloroethanol, triethylamine (TEA), triethanolamine (TEOA), DMF, and NEt_4Cl were obtained from Aldrich.

Elemental analyses were carried out on a Leco, CHNS-932 instrument. FT-IR spectra were recorded on an FT-IR JASCO 680-PLUS spectrometer. ^1H and ^{13}C-{^1H} NMR spectra were recorded on a Bruker Avance III-400 NMR spectrometer at 298 K. The UV–Vis spectra were recorded on a JASCO-570 spectrophotometer. Fluorescence spectra were recorded with a

JASCO FP-750 spectrofluorometer at room temperature in DMF. Gas chromatograms were recorded with a Varian STAR 3400 gas chromatograph with He as the carrier gas.

All photocatalytic reactions were performed in a quartz test tube (i.d. = 12 mm; 18 mL volume) containing 10 mL DMF/TEA (4:1 v/v), DMF/TEOA (4:1 v/v), or DMF/TEOA/NEt_4Cl (4:1 v/v, containing 10 mg NEt_4Cl) solution of the Re(I) complex (2×10^{-4} M) after bubbling through with pure CO_2 for 20 min at room temperature. The CO_2 concentration in solutions is about 0.2 M at 0.1 MPa and 25ºC. Each sample solution was irradiated by a high-pressure mercury lamp with a 365 nm band-pass filter for 0–24 h with stirring. The temperature of the reaction solution was maintained at 25 ± 2ºC by a fan cooling system during the irradiation process. The intensity of the mercury lamp was determined using a standard actinometer $K_3[Fe(C_2O_4)_3]$. After each irradiation step, a gas sample was taken using a gas-tight syringe and the produced CO gas was detected by gas chromatograph (GC). In all experiments, only CO gas with no detectable quantity of H_2 gas was found in the headspace of the reaction vessels. The irradiation of the tricarbonyl Re(I) complex with UV rays of 365 nm may lead to photodissociation and photodecomposition reactions. In addition, the irradiation of one *fac*-[Re(phen-dione)$(CO)_3Cl$] molecule may release three CO molecules in the absence of CO_2 atmosphere ([Re(phen-dione)$(CO)_3Cl$] → [Re(phen-dione)$(solvent)_3Cl$] + 3CO) . To confirm the stability of [Re(phen-dione)$(CO)_3Cl$] in the DMF/TEA, DMF/TEOA, and DMF/TEOA/NEt_4Cl solutions at room temperature, a UV–Vis study was performed under conditions similar to those used for the photocatalytic reactions in the absence of CO_2 atmosphere. The spectral features of *fac*-[Re(phen-dione)$(CO)_3Cl$] exhibited no change in the position of absorption bands over a period of 24 h under irradiation of the UV lamp (365 nm), and no precipitation or turbidity was observed even after long storage at room temperature (at least 4 weeks after preparation). Also, no detectable quantity of CO gas was found in the headspace of the blank solutions (the solutions of [Re(phen-dione)$(CO)_3Cl$] in the DMF/TEA, DMF/TEOA, or DMF/TEOA/NEt_4Cl mixture without CO_2 added) after irradiation at 365 nm for 24 h. This suggests that the Re(I) complex is completely stable under the experimental conditions.

2.2. Synthesis of *fac*-[Re(phen-dione)$(CO)_3Cl$]

Although, the synthesis of *fac*-[Re(phen-dione)$(CO)_3Cl$] has previously reported[13], here this complex was prepared according to a new method with a high yield (78%). In a typical experiment, a mixture of 210 mg (0.322 mmol) of $Re_2(CO)_{10}$ and 162 mg (0.766 mmol) of phen-dione was refluxed in 35 mL of 2-chloroethanol for 12 h under N_2 atmosphere, during which time the color of the reaction mixture changed from pale yellow to orange. After being cooled to room temperature, the solution was filtered and evaporated to dryness to give an orange residue. The purification of the crude product was carried out by column chromatography (Al_2O_3, grade III, WA, 30 × 1 cm column). Elution with chloroform/toluene (1:1 v/v) gave a yellow band of the pure complex, which was collected, evaporated to dryness, and then recrystallized by slow evaporation of a CH_2Cl_2–hexane (1:1 v/v) solution of the complex at 5ºC. The microcrystals of the Re(I) complex were collected by filtration. Yield: 260 mg (78 %). Elemental Anal. Calcd. for $C_{15}H_6ClN_2O_5Re$: C, 34.98; H, 1.18; N, 5.41. Found: C, 35.14; H, 1.17; N, 5.38%. IR (KBr; ν_{max}/cm^{-1}): CO = 2100 (s), 1920, 1850 (s); phen-dione = 1700 (m), 1680 (w), 1570 (m), 1457 (w), 1412 (w), 1111 (w), 810 (w), 737 (w). UV–Vis (DMF; λ/max, nm (ε, M^{-1} cm^{-1}): 270 (9860), 308 (5789), and 365 (2500). ^1H NMR (δ (ppm), DMSO-d_6): 9.03 (dd, 2 H), 8.58 (dd, 2 H), 8.05 (dd, 2 H). ^{13}C-{^1H}NMR (δ (ppm), DMSO-d_6): 188.5–197 (s, $C_{carbonyl}$), 173 (s, $C{=}O_{phen\text{-}dione}$) 136.3–165 (s, $C_{pyridyl}$).

2.3. Computational details

All calculations were carried out using the GAUSSIAN 09 suite of programs[14] and Mopac 2007 software. The geometrical structures of the considered complexes involved in the photocatalytic cycles were fully optimized without any symmetry restrictions in both gas and solution phases using the PM7 semi-empirical method implemented in Mopac 2007 software. The COSMO method was used for modeling the solvent in optimizing the structures in DMF. The calculated optimized structures in the gas and solution phases were used for frequency calculation at the DFT method using M062X functional.[15] 6-31+G(d) basis set for C, H, N and Cl; and the effective core potential, LANL2DZ, for Re were used for the frequency calculations. The SMD model[16] was used for modeling the solvent in the frequency calculation. To calculate the free energy solvation of the structures involved in the photocatalytic cycles in DMF, a thermodynamic cycle presented in Scheme 6 was used. Also, the dipole moment, energies of the frontier molecular orbitals (FMOs), and atomic charges were determined at the same level of theory.

3. Results and Discussion

3.1. Synthesis

The synthesis strategy for the Re(I) complex is summarized in Scheme 3. The complex was synthesized by reacting $Re_2(CO)_{10}$ with 1, 10-phenanthroline-5,6-dione (phen-dione) in dry 2-chloroethanol under a nitrogen atmosphere. The complex was purified by column chromatography.

No investigation was performed on the mechanism of the synthesis of [Re(phen-dione)$(CO)_3Cl$]. Although the synthesis of *fac*-[Re(phen-dione)$(CO)_3Cl$] has been previously reported [13], the reaction yield was low. In addition, our synthesis method is totally different and has a higher reaction yield and a shorter reaction time. In the previous method, the Re precursor is $Re(CO)_5Cl$, but in this paper, $Re_2(CO)_{10}$ is the starting complex and the origin of the chloro ligand is solvent 2-chloroethanol ($ClCH_2CH_2OH$). The following reaction can be proposed to account for the formation of the Re–Cl bond in 2-chloroethanol (eqn 1). [17]

$$Re_2CO_{10} + 2\,(\text{diimine}) + 2\,\text{Cl-}CH_2CH_3OH \longrightarrow \qquad (1)$$

$$2\,\textit{fac}\text{-}[Re(\text{diimine})(CO)_3Cl] + CH_3CH_2OH + 4\,CO + ClCH_2CHO$$

3.2. Photophysical properties

The absorption spectrum of the complex in DMF (5.7×10^{-5} M) at room temperature is depicted in Fig. 1. The complex shows two intense absorption bands at 270 ($\varepsilon = 9860\ M^{-1}\ cm^{-1}$) and 308 nm ($\varepsilon = 5789\ M^{-1}\ cm^{-1}$) that can be assigned to the spin-allowed intraligand ($\pi \rightarrow \pi^*$) transitions. By contrast, the broad band at 365 nm ($\varepsilon = 2500\ M^{-1}\ cm^{-1}$) is attributed to the $d\pi_{(Re(I))} \rightarrow \pi^*_{(\text{phen-dione})}$, metal-to-ligand charge-transfer (MLCT) transition.[18,19] The emission spectrum of the complex at room temperature is shown in Fig. 2. When the complex was excited at 365 nm, a broad emission band was appeared at 570 nm.

The IR spectrum of the complex contains three strong v (CO) absorption bands at 2100, 1920, and 1850 cm^{-1} which confirms a *facial* geometry (*fac*) for three CO ligands in the complex. Generally, a *facial* isomer has three intense bands in the carbonyl region, although the *meridional* isomer (*mer*) has only two intense bands.[20] The bands around 1700–1400 cm^{-1} are assigned to the stretching of the phen-dione rings.

3.3. NMR studies

The rhenium(I) complex was characterized using ^{1}H and ^{13}C NMR techniques in DMSO-d_6. The aromatic region of the ^{1}H NMR spectrum is integrated for 6 protons, as expected for coordinated pyridyl rings, including three different pairs of protons. The ^{13}C NMR shows the difference between $C_{carbonyl}$, $C_{pyridyl}$, and $C{=}O_{phen\text{-}dione}$ very well. The ^{1}H and ^{13}C NMR data of the complex are given in the experimental section.

3.4. Photocatalytic reduction of CO_2 to CO

The photocatalytic experiments were performed in three CO_2-saturated solutions of the complex (2×10^{-4} M) in DMF/TEA (4:1 v/v), DMF/TEOA (4:1 v/v), or DMF/TEOA/NEt_4Cl (4:1 v/v containing 10 mg NEt_4Cl) mixture under UV radiation of 365 nm at room temperature. TEA and TEOA are sacrificial donors; and NEt_4Cl is a free chloride source. In the solution of the complex in DMF/TEOA mixture, 27 μmol of CO was produced after 24 h of irradiation, whereas only 25.5 μmol of CO was formed in DMF/TEA mixture under the same conditions. Addition of an excess amount (10 mg) of NEt_4Cl (as a chloride source) to the DMF/TEOA mixture increases the moles of produced CO to 34 μmol (Fig. 3). The turnover number for the formation of CO (TN_{CO}: based on the complex concentration (TN_{CO} = (mol of CO at 24 h)/(mol of the catalyst)) in this research is comparable with similar complexes.[21] The turnover numbers for the formation of CO were 12.8, 13.5, and 17 using DMF/TEA, DMF/TEOA, and DMF/TEOA/NEt_4Cl solutions, respectively.

3.5. Theoretical calculations

3.5.1 Theoretical evaluation of the proposed photocatalytic cycles

The reduction mechanism of CO_2 to CO by *fac*-[Re(phen-dione)$(CO)_3$Cl] complex was presented by two different routes and evaluated by theoretical calculations. The steps of the considered routes are shown in Scheme 3. It should be mentioned that the photoexcitation step of each route has not been considered in the calculations. The structures of all species in their ground electronic states, involved in two routes, were separately optimized in both gas and solution (DMF) phases. The calculation of the excited state of the catalyst in the catalytic cycle (Scheme 3) is not necessary because all of the species in the cycle are in their ground electronic states. Although, there is one photo-excitation process in the cycle, but the triplet metal-to-ligand charge transfer (^{3}MLCT) excited state reacts with Et_3N and accepts one electron to achieve a stable state **(Int1)** in its ground electronic state. The optimized geometries for the species involved in the proposed mechanisms in both gas and solution phases are shown in Schemes 4 and 5, respectively. The distribution and energy of the FMOs of these species are shown in Figs. 4 and 5 for both gas and solution phases, respectively.

3.5.2 Thermodynamic cycle

The calculated standard (298 K and 1 bar) Gibbs free energies (G^o, in Hartree) and the solvation Gibbs free energy (ΔG^o_{solv}, kcal mol^{-1}) for each species are listed in Table 1. Table 2 summarizes the gas-phase Gibbs free energy change (ΔG^o, kcal mol^{-1}) of each step in the proposed catalytic cycles in both gas and solution phases.

The gas-phase Gibbs free energy change (ΔG^o_{gas}) is calculated using eqn 2 (A is a reactant, and B and C are products, for a supposed reaction which take places in the standard condition).

$$\Delta G^o_{gas} = G^o_{gas}(B) + G^o_{gas}(C) - G^o_{gas}(A) \qquad (2)$$

According to the thermodynamic cycle shown in Scheme 6,[22] the term ΔG_g is the gas-phase free energy change of the reaction and the term ΔG_{sol} is the desired free energy change in solution which is calculated using eqn 3.

$$\Delta G_{sol} = \Delta G_{gas} - \Delta G^{A}_{sol} + \Delta G^{B}_{sol} + \Delta G^{C}_{sol} \qquad (3)$$

Three other parts, ΔG^{A}_{sol} , ΔG^{B}_{sol}, and ΔG^{C}_{sol} are the free energy of solvation of the reactant (A) and the products (B and C), respectively.

3.5.3 Mechanism

As shown in Scheme 3, the OER rhenium **Int1** is an initiator which can start the mechanisms. This intermediate is formed by the photoexcitation of the **Catalyst** through incident light where the excitation of the Re(I) complex is related to the triplet metal-to-ligand charge-transfer (^{3}MLCT) which is quenched by triethylamine (TEA, **10**) as a sacrificial donor. The ^{3}MLCT excited state of the complex is assigned to a $d\pi_{(Re(I))} \rightarrow \pi^*_{(phen\text{-}dione)}$ transition[19]. As shown in Fig. 6, the HOMO of *fac*-[Re(phen-dione)(CO)$_3$Cl] demonstrates a $d\pi$ metal character in the gas phase. A relatively minor contribution to these occupied orbitals is also clear from the chloro and carbonyl ligands. In addition, the calculated LUMO is mainly composed by the phen-dione ligand and is primarily π^* in character. The calculated results show that the localization of the HOMO of the complex in solution is different to what was seen in the gas phase (see Fig. 6), which has direct relation with the spectroscopic and photophysical properties of polypyridyl rhenium complexes.[23] It is seen that the HOMOs of the Re complex in the solution phase (DMF) is characterized by the localization of electron densities on the phen-dione ligand, while a major contribution to the LUMO is presented from Re center. In this case, the ^{3}MLCT transition can be occurred from the HOMO –1 orbital to the LUMO +1 orbital in the solution phase. This photoexcitation generates a radical ion pair **Int1** and $Et_3N^{\bullet+}$ (**11**). Similarly, due to the photochemical reaction, the TEOA$^{\bullet+}$ radical cation is formed by an electron transfer from triethanolamine (TEOA) to the excited Re(I) complex at the same conditions.[4c] An important step for both cycles shown in Scheme 3 is a proton transfer from $[Et_3N]^{\bullet+}$ (**11**) to another molecule of Et_3N (**10**) and generates a neutral radical $CH_3C^{\bullet}HNEt_2$ (**12**) along with a cation Et_3NH^+ (**13**) (step **Ib**),[11*d*] which may act as a radical reducing agent and a proton source, respectively. The proton concentration increases with the Et_3N decomposition process. The dissociation of the radical anion **Int1** yields a chloride anion (**14**) as well as a rhenium radical **Int2** with a vacant coordination site at the axial position. **Int2** has a five–coordinate structure. This process is entropically favored, because one species converts to two species but, the theoretical calculations show that this process is not a significant spontaneous step in the solution phase ($\Delta G^{o}_{sol} = -0.088$ kcal mol^{-1}). Comparing this value with the corresponding value reported in Table 2 in the gas phase shows that the solvent has considerable effect in changing the value of ΔG^{o}_{g} of this reaction from positive to negative. In the five–coordinate structure, there is a vacant coordination site at the axial position which can be used for coordination of a solvent molecule (DMF). The radical **Int2** rapidly converts to the DMF–coordinated radical complex **Int3**. At this point, adduct of CO_2 to **Int3** yields a CO_2–coordinated **Int4** from the DMF–coordinated Re complex. The newly formed Re–C bond between the rhenium moiety and the adducting CO_2 in step **III,** constitutes an intermediate **Int4**. In our investigation, the computational results have indicated that the C–bonded (Re–C) **Int4** is preferred to the O–bonded (Re–O) isomer**.** Thus, the Re–C bond formation is more favor compared to the Re–O bond. At the moment of the adduct of CO_2 to Re(I) center, there is a remarkable change in the CO_2 geometry from the linear form to the bent form in which the O–C–O angle decreases from 180.000° to 171.957 and 134.339° in the gas and solution phases, respectively. As a result, there is an increase in the C–O distances; the C–O bond length varies from 1.17023 Å in free CO_2 molecule, to 1.21857 and 1.22330 Å in **Int4** at the solution phase. In addition, it should be mentioned that the value of free energy changes of step **III** is the highest value among the other values reported in Table 2 in DMF. The reaction of **Int4** with a proton gives a metal carboxylate **Int5**. A new outer–sphere electron transfer to $[Re(phen–dione)(CO)_3(COOH)]^{\bullet+}$ yields OH^- (**17**) and **Int6**: $[Re(phen–dione)(CO)_4]^+$.

On the basis of previous study,[12] after the electron transfer from **Int1** or radical **12** ($CH_3C^{\bullet}HNEt_2$) to $[Re(phen–dione)(CO)_3(COOH)]^{\bullet+}$ (**Int 5**) and the dehydroxylation reaction in step **V** (Scheme 3), "the other O atom" of CO_2 yields a hydroxide anion (OH^-). Also, Gibson and co-workers[4d] afforded to study of photocatalytic reduction reaction of *fac*-$[Re(dmbpy)(CO)_3Cl]$ with CO_2 which is generated *fac*-$[Re(dmbpy)(CO)_3COOH]$. Their findings have shown that the Re-carboxylate complex converts to $[Re(dmbpy)(CO)_3]^+$ and OH^-. The OH^- and Et_3NH^+ ions undergo a neutralization reaction to generate H_2O and Et_3N.[5d] Also, the hydroxide anion can react with dissolved CO_2 in DMF solution and produce a bicarbonate anion ($OH^- + CO_2 \rightarrow HCO_3^-$). With inclusion of solvation, the step **IV** is predicted by our calculations (Table 2) to be nonspontaneous by +30.51 kcal mol^{-1}, while the dehydroxylation reaction in step **V** is spontaneous by –82.29 kcal mol^{-1}. Since the formation of a CO molecule from CO_2 requires a 2–electron reduction of CO_2, another electron in step **VI** should be necessary for the reduction of CO_2, which is inputted into the 17–ē species generated by the loss of the chloro ligand from the OER species or the CO_2 adduct.[24] According to Ishitani et al.,[7] the OER species (**Int1**) itself has strong reducing power ($E_{1/2} = -1.61$ V *vs.* $Ag/AgNO_3$); or the radical reducing agent **12** ($CH_3C^{\bullet}HNEt_2$) formed through step **Ib**,[25] which are possibly the second electron sources. The dissociation of **Int6** yields a CO molecule (**18**) and a rhenium cation **Int7**. This step is comparatively spontaneous by −6.40 kcal mol^{-1} in the solution phase. Previous papers have reported that the rhenium cation **Int7** may then follow two potential pathways: one leading to regenerates **Catalyst** through a reassociation reaction of **Int7** with a chloride anion (**14**) (step **VII**: +2.83 kcal mol^{-1}, Scheme 3) and the other to transform into the DMF–coordinated rhenium cation **Int8**, without the replacement of Cl$^-$ (step **VIII**: +24.65 kcal mol^{-1}, Scheme 3). The DMF–coordinated Re cation **Int8** absorbs UV radiation to form the one–electron–reduced (OER) DMF–coordinated radical **Int3**, driving the continuous reaction cycle. The possibility of reaction progress through **VII** or **VIII** step has been debated in the literatures. In some cases, the increase of the lifetime of the OER **Int1**[7] and CO formation by addition of an excess X$^-$ using [Re(diimine)(CO)$_3$X][26] is one of the reasons for improvement of regeneration of the **Catalyst** through step **VII**. Also, Inoue et al.[12] have studied the photochemical reduction of CO$_2$ catalyzed by [Re(dmbpy)(CO)$_3$Cl], they detected the DMF–coordinated Re complex ([Re(dmbpy)(CO)$_3$(DMF)]) and CO$_2$–coordinated Re complex ([Re(dmbpy)(CO)$_3$(COOH)]). They proposed that a photochemical reduction of CO$_2$ must occur through an intermediate similar to DMF–coordinated Re cation **Int8** (step **VIII**). The DFT calculations reveal that the catalytic cycles in the gas phase and with inclusion of solvation through step **VII** has a significant driving force (–23.26 and –24.32 kcal mol^{-1} in the gas and solution phases, respectively), while the formation of the DMF–coordinated rhenium cation **Int8** through step **VIII** is not very thermodynamically favorable (+80.33 and –0.66 kcal mol^{-1} in the gas and solution phases, respectively). The results also show that both possibility of reaction progress through step **VII** or **VIII** with inclusion of solvation are thermodynamically feasible, although the regeneration of **Catalyst** through step **VII** is much more suitable. The CSI-MS measurements of the reaction mixture and FT-IR studies[12] have provided clear evidence for the formation of the

DMF–coordinated Re cation similar to **Int8** through step **VIII**. Finally, we can conclude that the catalytic cycle for CO_2 reduction through step **VIII** is much more kinetically desirable.

Conclusions

We have reported here a new method for the preparation of a mononuclear Re(I) phen-dione complex, *fac*-[Re(phen-dione)$(CO)_3$Cl] and its application as a photocatalyst for the photochemical reduction of CO_2 to CO. According to the theoretical calculations, two catalytic pathways for the reduction of CO_2 to CO were proposed. The proposed pathways are consistent with the experimental findings by Ishitani and Inoue. Actually, we have proposed the photocatalytic mechanism according to the formation of CO as the final product which was detected in the experimental section. It's worthy to mention that, only CO gas with no detectable quantity of H_2, formic acid, MeOH, or CH_4 was found in the reaction mixture after irradiation. Also, the addition of an excess amount of NEt_4Cl (as a chloride source) to the DMF/TEOA mixture increases the formation of CO. Since the reduction of CO_2 to CO requires two electrons in step **V** in the proposed mechanism, another electron should be supplied by a strong reducing agent. According to Ishitani's studies, the OER species (**Int1**) acts as a reducing agent. Therefore, it can be confirmed the photoexcitation step and the dehydroxylation step (step **V**) occur in the solution. The formation of **Int1** and radical **12** is increased when the excess chloride source NEt_4Cl is added to the reaction mixture. As can be shown in Scheme 3, **Int1**and radical **12** can act as a potential reducing agent. In addition, the polar solvent DMF (which was used in the experimental section) is a suitable ligand for the formation of solvent-coordinated Re(I) in steps **II** and **VIII** (Scheme 3).

The theoretical calculations were demonstrated both cycles for photochemical reduction of CO_2 to CO in the presence of the Re(I) complex were thermodynamically possible. Although, the regeneration of the initial **Catalyst**, *fac*-[Re(phen-dione)(CO)$_3$Cl], through a reassociation reaction with a chloro ligand is much more suitable. Also, the catalytic cycle for CO$_2$ reduction through step **VIII** is much more kinetically desirable.

Acknowledgements

We are grateful to the Iran National Science Foundation (INSF) (Project No. 90006991) and Isfahan University of Technology (IUT) for financial support.

References

1 A. J. Morris, G. J. Meyer and E. Fujita, *E. Acc. Chem. Res.*, 2009, **42**, 1983–1994.

2 W. Leitner, *Coord. Chem. Rev.*, 1996, **153**, 257–284.

3 (*a*) K. Ikeue, H. Yamashita, M. Anpo and T. Takewaki; *J. Phys. Chem. B*, 2001, **105**, 8350–8355; (*b*) A. Khenkin, I. Efremenko, L. Weiner, J. Martin and R. Neumann, *Chem. Eur. J.*, 2010, **16**, 1356–1364; (*c*) C. Creutz, H. A. Schwarz, J. F. Wishart, E. Fujita and N. Sutin, *J. Am. Chem. Soc.*, 1991, **113**, 3361–3371; (*d*) E. Simón-Manso and C. P. Kubiak, *Organometallics*, 2005, **24**, 96−102; (*e*) H. Ishida, T. Terada, K. Tanaka ans T. Tanaka, *Organometallics*, 1990, **6**,181–186.

4 (*a*) B. Gholamkhass, H. Mametsuka, K. Koike, T. Tanabe, M. Furue and O. Ishitani, *Inorg. Chem.*, 2005, **44**, 2326–2336; (*b*) J. Shakeri, H. Hadadzadeh and H. Tavakol, *Polyhedron*, 2014, **78**, 112–122; (*c*) C. Bruckmeier, M. W. Lehenmeier, R. Reithmeier, B. Rieger, J. Herranz and C. Kavakli, *Dalton Trans.*, 2012, **41**, 5026–5037; (d) D. H. Gibson, X. Yin, H. He, and M. S. Mashuta, *Organometallics*, 2003, **22**, 337−346;

5 (*a*) W. Kaim and S. Kohlmann, *Chem. Phys. Lett.*, 1987, **139**, 365–369; (*b*) D. J. Stufkens,

Inorg Chem., 1992, **13**, 359–369; (*c*) Y. Hayashi, S. Kita, B. S. Brunschwig and E. Fujita, *J. Am. Chem. Soc.*, 2003, **125**, 11976–11987; (*d*) B. Kumar, M. Llorente, J. Froehlich, T. Dang, A. Sathrum, and C. P. Kubiak, *Annu. Rev. Phys. Chem*. 2012. **63**, 541–569; (*e*) Y. Yan, E. L. Zeitler, J. Gu, Y. Hu, and A. B. Bocarsly, *J. Am. Chem. Soc.*, 2013, **135**, 14020-14023; (*f*) J. A. Keith, K. A. Grice, C. P. Kubiak, and E. A. Carter, *J. Am. Chem. Soc.*, 2013, **135**, 15823- 15829; (*g*) C. Riplinger, and E. A. Carter *ACS Catal.*, 2015, **5**, 900–908; (*h*) M. V. Vollmer, C. W. Machan, M. L. Clark, W. E. Antholine, J. Agarwal, H. F. Schaefer, C. P. Kubiak, and J. R. Walensky, *Organometallics*, 2015, **34**, 3–12.

6 J. Hawecker, J. M. Lehn and R. Ziessel, *J. Chem. Soc., Chem. Commun.*, 1983, 536–538.

7 H. Takeda, K. Koike, H. Inoue and O. Ishitani, *J. Am. Chem. Soc.*, 2008, **130**, 2023–2031.

8 P. Kurz, B. Probst, B. Spingler, and R. Alberto, *Eur. J. Inorg. Chem.*, 2006, **15**, 2966–2974

9 J. M. Smieja, M. D. Sampson, K. A. Grice, E. E. Benson, J. D. Froehlich and C. P. Kubiak, *Inorg. Chem.*, 2013, **52**, 2484–2491.

10 E. E. Benson, K. A. Grice, J. M. Smieja and C. P. Kubiak, *Polyhedron*, 2013, **58**, 229–234.

11 (*a*) J. Agarwal, B. C. Sanders, E. Fujita, H. F. Schaefer, T. C. Harrop and J. T. Muckerman, *Chem. Commun.*, 2012, **48**, 6797–6799; (*b*) T. Morimoto, T. Nakajima, S. Sawa, R. Nakanishi, D. Imori and O. Ishitani, *J. Am. Chem. Soc.*, 2013, **135**, 16825–16828; (*c*) J. Agarwal, E. Fujita, H. F. Schaefer, and J. T. Muckerman, *J. Am. Chem. Soc.*, 2012, **134**, 5180–5186; (*d*) J. Agarwal, R. P. Johnson, and G. Li, *J. Phys. Chem. A*, 2011, **115**, 2877–2881; (*e*) F.H. Haghighi, H. Hadadzadeh, H. Farrokhpour, N. Serri, Kh. Abdi and H.A. Rudbari, *Dalton Trans.*, 2014, **43**, 11317–11332.

12 Y. Kou, Y. Nabetani, D. Masui, T. Shimada, S. Takagi, H. Tachibana, and H. Inoue, *J. Am. Chem. Soc.*, 2014, **136**, 6021–6030.

13 (*a*) M. Wrighton and D. L. Morse, *J. Am. Chem. Soc.*, 1974, **96**, 998–1003; (*b*) H. D. Stoeffler, N. B. Thornton, S. L. Temkin, and K. S. Schanze, *J. Am. Chem. Soc.*, 1995, **117**, 7119–7128.

14 M. J. Frisch, G. W. Trucks, H. B. Schlegel, G. E. Scuseria, M. A. Robb, J. R. Cheeseman, G. Scalmani, V. Barone, B. Mennucci, G. A. Petersson, H. Nakatsuji, M. Caricato, X. Li, H. P. Hratchian, A. F. Izmaylov, J. Bloino, G. Zheng, J. L. Sonnenberg, M. Hada, M. Ehara, K. Toyota, R. Fukuda, J. Hasegawa, M. Ishida, T. Nakajima, Y. Honda, O. Kitao, H. Nakai, T. Vreven, J. A. Montgomery Jr., J. E. Peralta, F. Ogliaro, M. Bearpark, J. J. Heyd, E. Brothers, K. N. Kudin, V. N. Staroverov, R. Kobayashi, J. Normand, K. Raghavachari, A. Rendell, J. C. Burant, S. S. Iyengar, J. Tomasi, M. Cossi, N. Rega, J. M. Millam, M. Klene, J. E. Knox, J. B. Cross, V. Bakken, C. Adamo, J. Jaramillo, R. Gomperts, R. E. Stratmann, O. Yazyev, A. J. Austin, R. Cammi, C. Pomelli, J. W. Ochterski, R. L. Martin, K. Morokuma, V. G. Zakrzewski, G. A. Voth, P. Salvador, J. J. Dannenberg, S. Dapprich, A. D. Daniels, O. Farkas, J. B. Foresman, J. V. Ortiz, J. Cioslowski and D. J. Fox, GAUSSIAN 09 (Revision A.01), Gaussian, Inc., Wallingford CT, 2009.

15 Y. Zhao, N. González-García, and D. G. Truhlar, *J. Phys. Chem. A*, 2006, **110**, 4942–4942.

16 (*a*) S. Miertus, E. Scrocco And J. Tomasi, *Chem. Phys.*, 1981, **55**, 117–129; (*b*) S. Miertus and J. Tomasi, *Chem. Phys.*, 1982, **65**, 239–245; (*c*) M. Cossi, V. Barone, R. Cammi and J. Tomasi, *Chem., Phys. Let.*, 1996, **255**, 327–335; (*d*) M. T. Cances, V. Mennucci and J. Tomasi, *J. Chem. Phys.*, 1997, **107**, 3032–3041; (*e*) V. Barone, M. Cossi, B. Mennucci and J. Tomasi, *J. Chem.*

Phys., 1997, **107**, 3210–3221.

17 (*a*) D. K. Orsa, G. K. Haynes, S. K. Pramanik, M. O. Iwunze, G. E. Greco, D. M. Ho, J. A. Krause, D. A. Hill, R. J. Williams and S. K. Mandal, *Inorg. Chem. Comm.*, 2008, **11**, 1054–1056; (*b*) G. Q. Li, J. Feldman, J. A. Krause and M. Orchin, *Polyhedron*, 1997, **16**, 2041–2045.

18 M.R. Waterland, T. J. Simpson, K. C. Gordon and A. K. Burrell, *J. Chem. Soc., Dalton Trans.*, 1998, 185–192.

19 L. Wallace and D. P. Rillema, *Inorg. Chem.*, 1993, **32**, 3836–3843.

20 (*a*) S. V. Wallendael, R. J. Shaver, D. P. Rillema, B. J. Yoblinshi, M. Stathis and T. F. Guarr, *Inorg. Chem.*, 1990, **29**, 1761–1767; (*b*) L.H. Staal, A. Oskama and K. Vrieze, *J. Organomet. Chem.* 1979, **170**, 235–245.

21 T. Yui, Y. Tamaki, K. Sekizawa and O. Ishitani, *Top. Curr. Chem.*, 2011, **303**, 151–184.

22 M. Abedi and H. Farrokhpour, *Dalton Trans.*, 2013, **42**, 5566–5572.

23 (*a*) G. Ferraudi, M. Feliz, E. Wolcan, I. Hsu, S. A. Moya and J. Guerrero, *J. Phys. Chem.* 1995, **99**, 4929–4936; (*b*) K. K. Lo, K. H. K. Tsang, W. K. Hui and N. Zhu, *Inorg. Chem.,* 2005, **44**, 6100–6109.

24 H. Takeda and O. Ishitani, *Coord. Chem. Rev.*, 2010, **254**, 346–354.

25 C. Kutal, M. A. Weber, G. Ferraudi and D. Geiger, *Organometallics*, 1985, **4**, 2161–2166

26 H. Hori, Y. Takano, K. Koike and Y. Sasaki, *Inorg. Chem. Comm.*, 2003, **6**, 300–303.

Table 1 Summary of $G^{o}_{(g)}$ (Gibbs free energies, in Hartree) and $\Delta G^{o}_{(solv)}$ (solvation Gibbs free energies, kcal mol^{-1})

Label	Structure	G^{o}(gas)	ΔG^{o}(solvation)
Catalyst	*fac*-[Re(phen-dione)(CO)$_3$Cl]	–1599.582465	–33.14
Int1	[Re(phen-dione)(CO)$_3$Cl]$^{\bullet-}$	–1599.698190	–51.26
Int2	[Re(phen-dione)(CO)$_3$]$^{\bullet}$	–1139.353627	–45.69
Int3	[Re(phen-dione)(CO)$_3$(DMF)]$^{\bullet}$	–1387.719252	–30.87
Int4	[Re(phen-dione)(CO)$_3$(CO$_2$)]$^{\bullet}$	–1327.855635	–30.23
Int5	[Re(phen-dione)(CO)$_3$(COOH)]$^{\bullet+}$	–1328.190883	–69.36
Int6	[Re(phen-dione)(CO)$_4$]$^{+}$	–1252.460332	–64.39
Int7	[Re(phen-dione)(CO)$_3$]$^{+}$	–1139.151815	–84.72
Int8	[Re(phen-dione)(CO)$_3$(DMF)]$^{+}$	–1387.486166	–63.10
10	Et$_3$N	–292.087395	–4.58
11	Et$_3$N$^{\bullet+}$	–291.807198	–57.53
12	CH$_3$C$^{\bullet}$HNEt$_2$	–291.447005	–4.51
13	Et$_3$NH^{+}	–291.807198	–59.71
14	Cl^{-}	–460.250162	–64.90
15	DMF	–248.326950	–7.67
16	CO$_2$	–188.524719	–1.39
17	OH^{-}	–75.744333	–78.61
18	CO	–113.290939	+2.90

Table 2 ΔG^{o}_{g} (gas-phase Gibbs free energy change, kcal mol^{-1}), and ΔG^{o}_{sol} (solution phase Gibbs free energy change, kcal mol^{-1}) of each step

Step	ΔG^{o}_{g}	ΔG^{o}_{sol}
Ia	+59.24	–0.09
Ib	+1.14	–0.97
II	–24.27	–1.76
III	+38.52	+32.87
IV	+14.51	+30.51
V	–8.65	–82.29
VI	+11.03	–6.40
VII	–113.65	+2.83
VIII	–4.64	+24.65

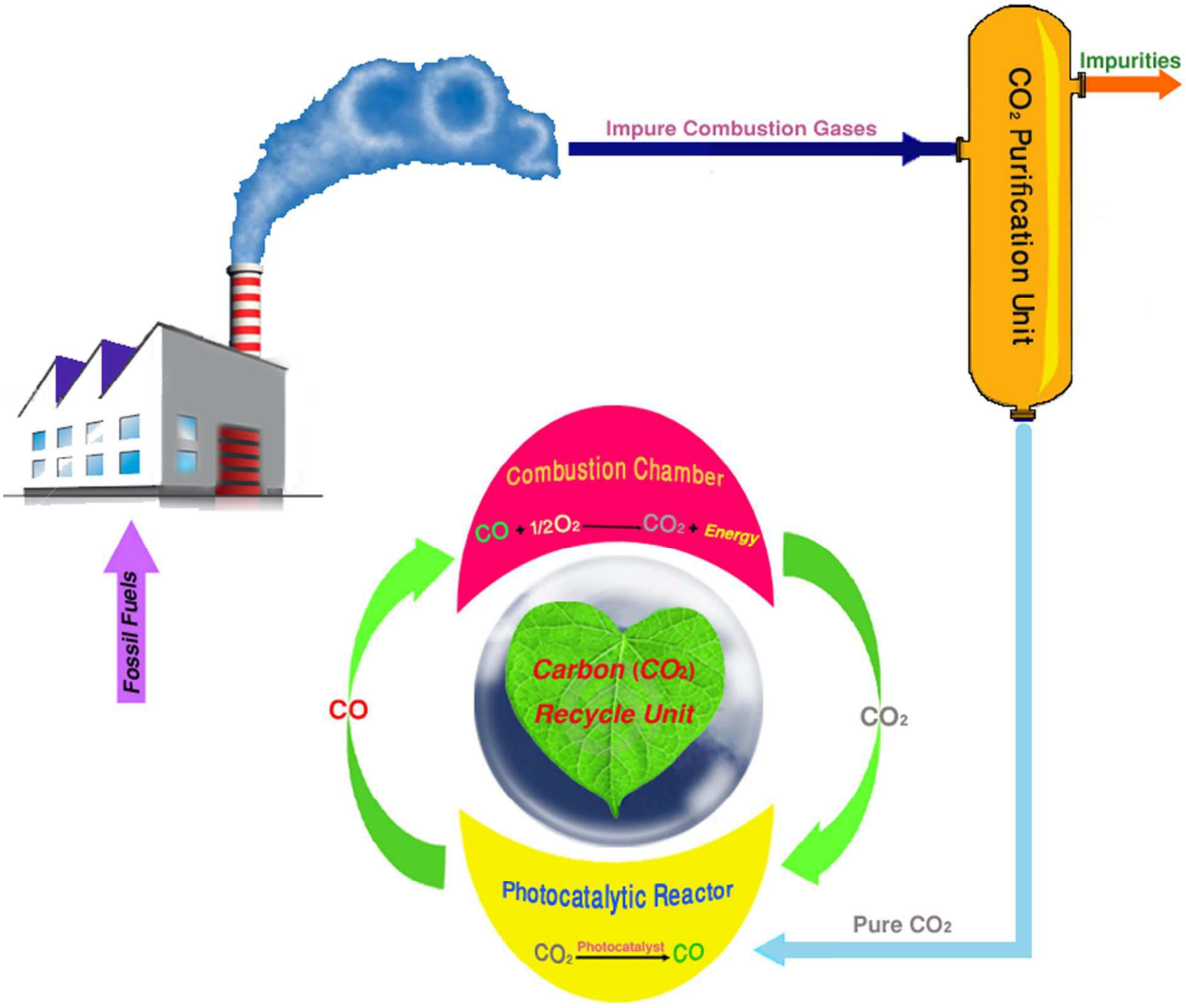

Scheme 1 Carbon (CO_2) recycle unit based on the photocatalytic reduction of CO_2 to CO.

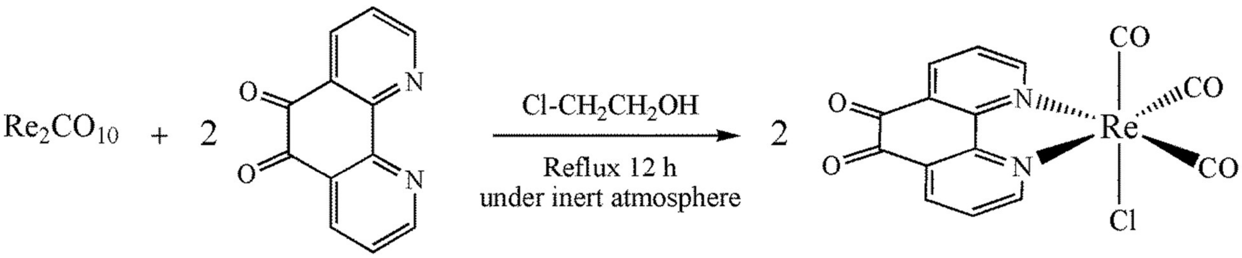

Scheme 2 Synthesis route to *fac*-[Re(phen-dione)$(CO)_3$Cl].

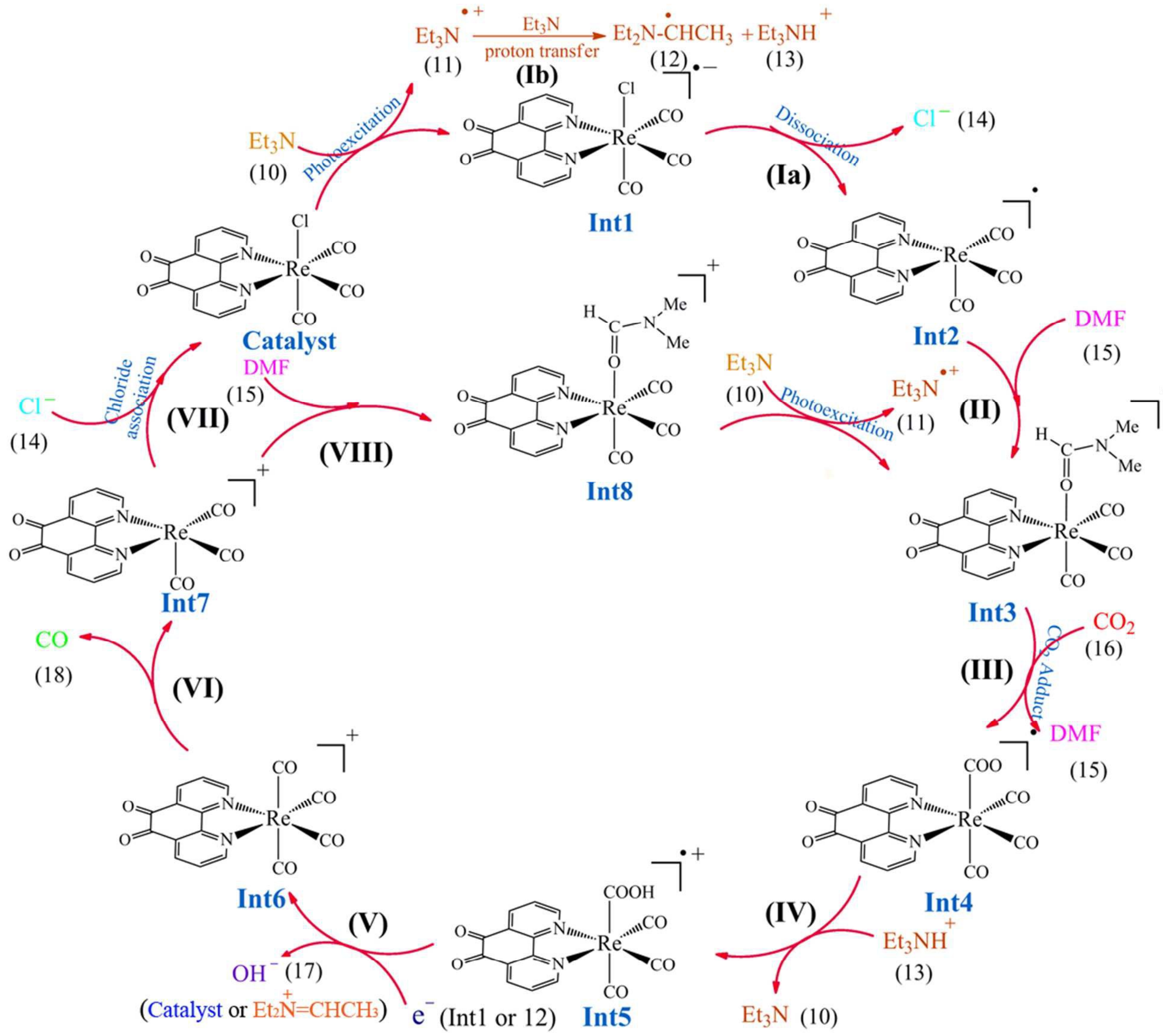

Scheme 3 The proposed reaction mechanism for the photocatalytic reduction of CO_2 to CO by the Re(I) complex.

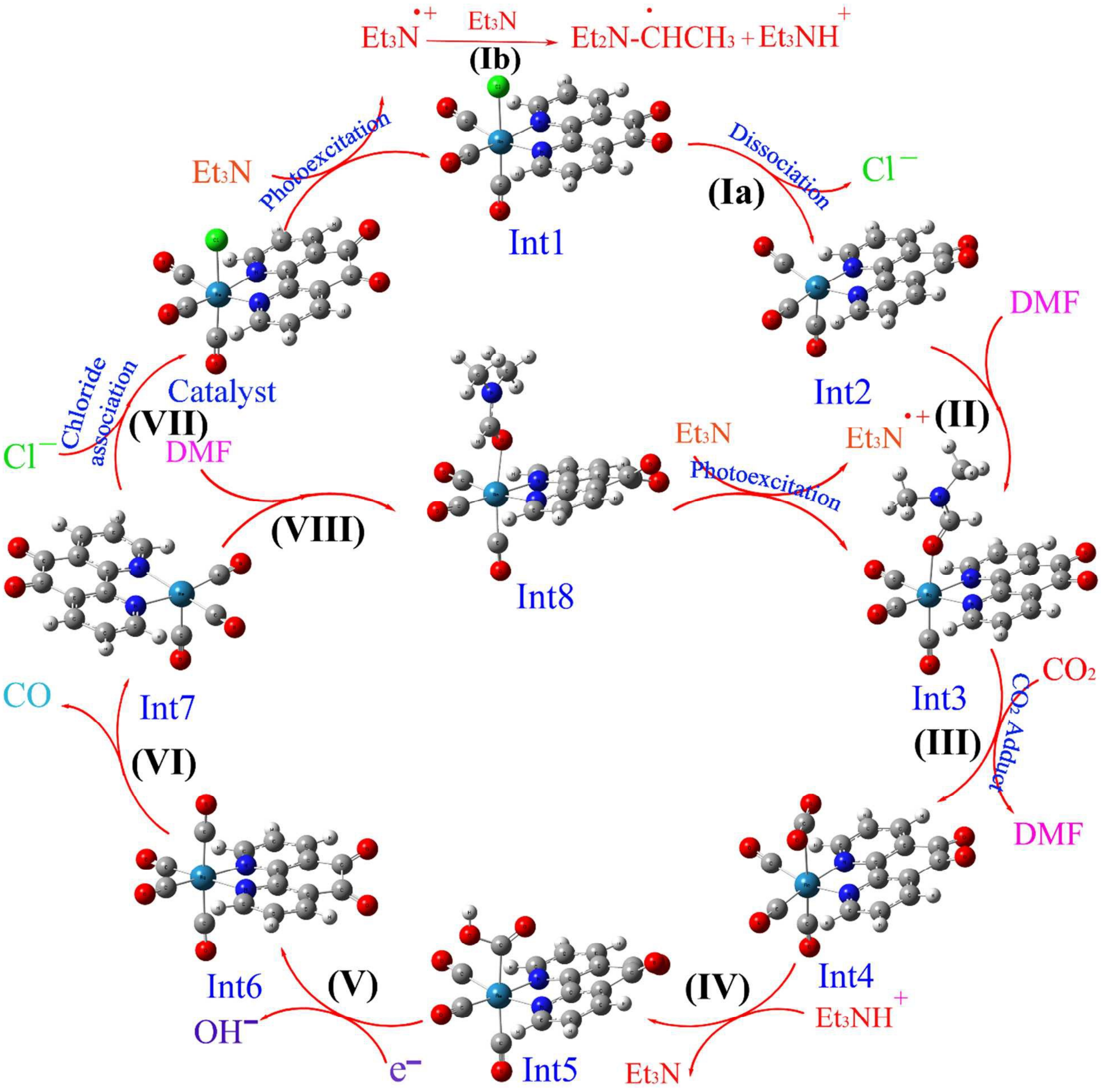

Scheme 4 The optimized structures of the species involved in the proposed mechanisms in the gas phase.

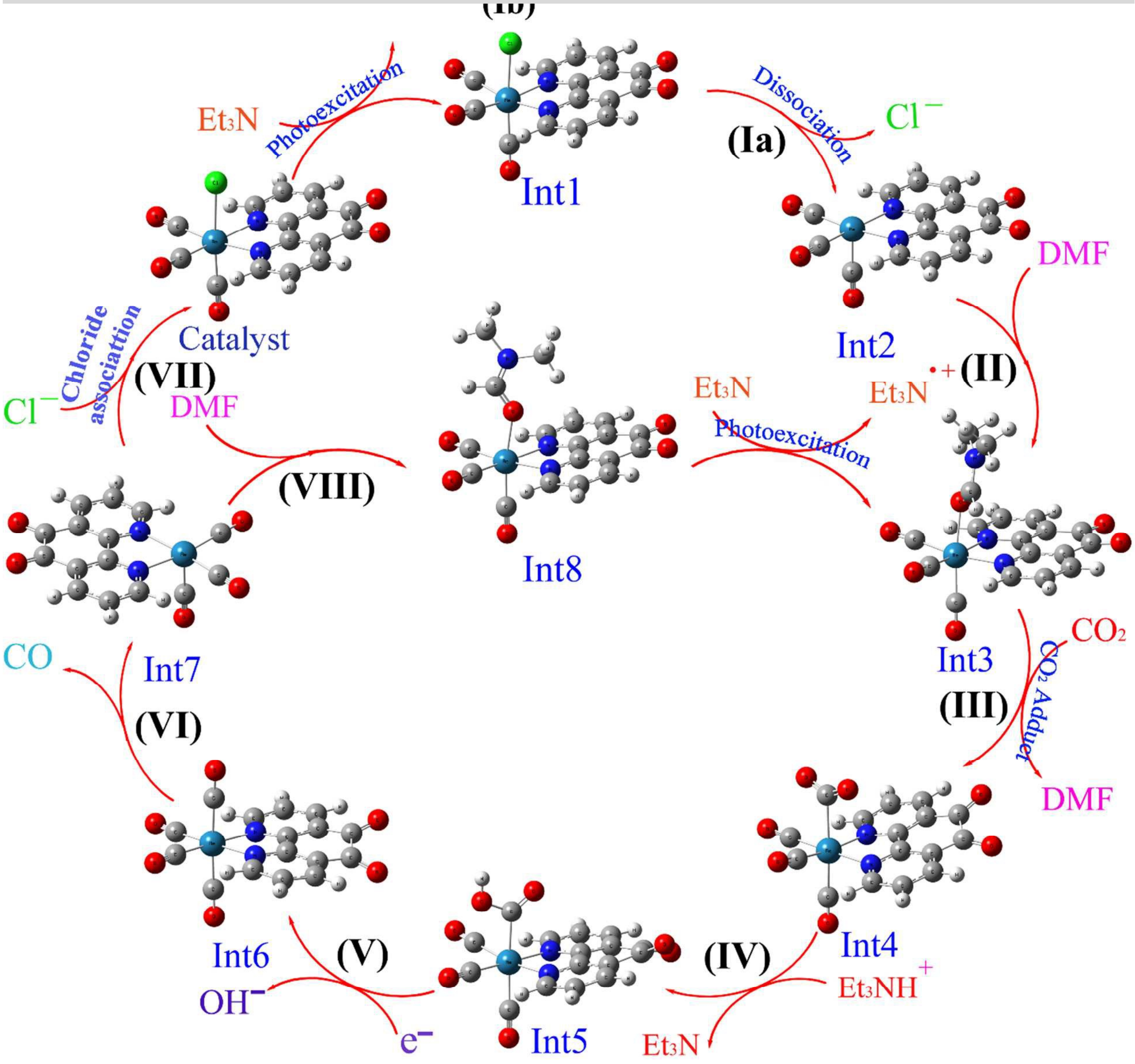

Scheme 5 The optimized structures of the species involved in the proposed mechanisms in the solution phase (DMF).

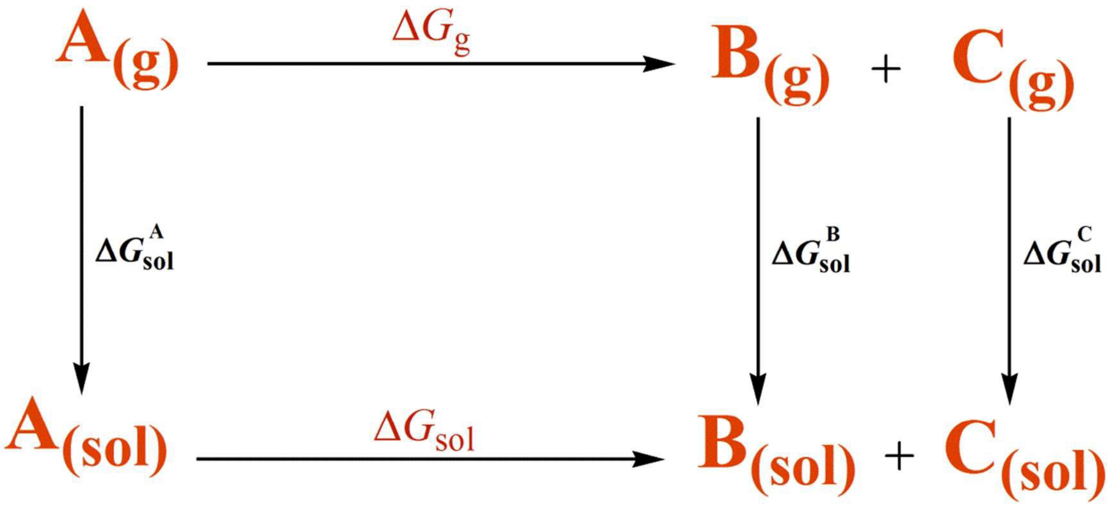

Scheme 6 Thermodynamic cycle for a typical reaction.

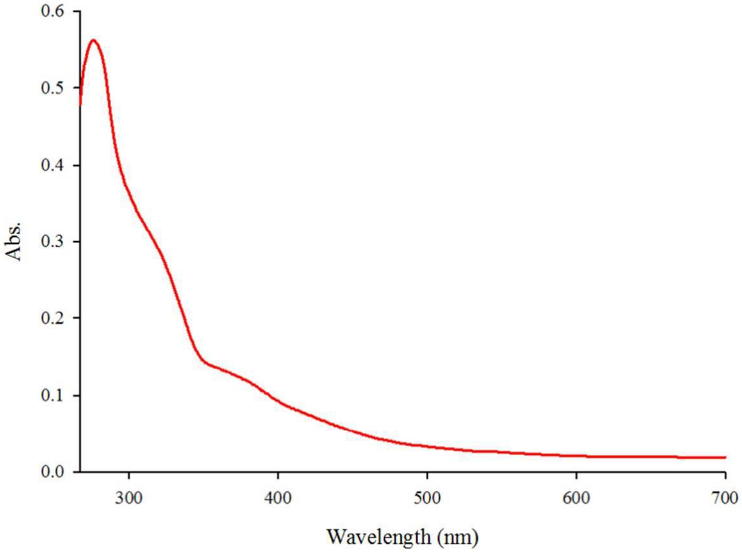

Fig. 1 The absorption spectrum of *fac*-[Re(phen-dione)(CO)$_3$Cl] in DMF solution (3.3 × 10^{-5} M).

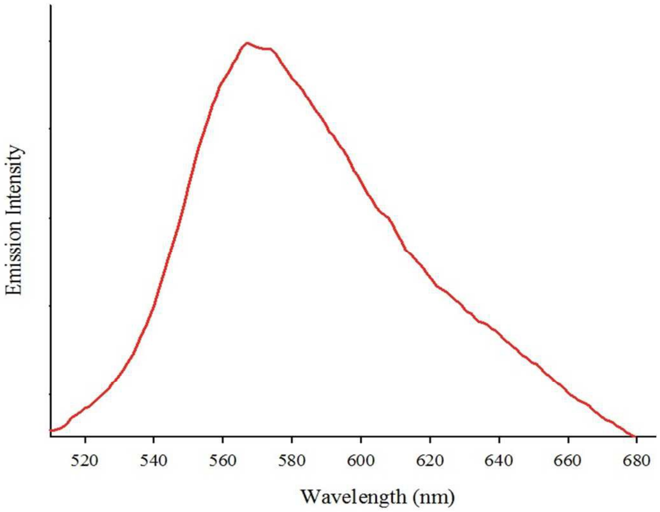

Fig. 2 The emissions spectrum of *fac*-[Re(phen-dione)(CO)$_3$Cl] at room temperature; λ_{ex} = 365 nm.

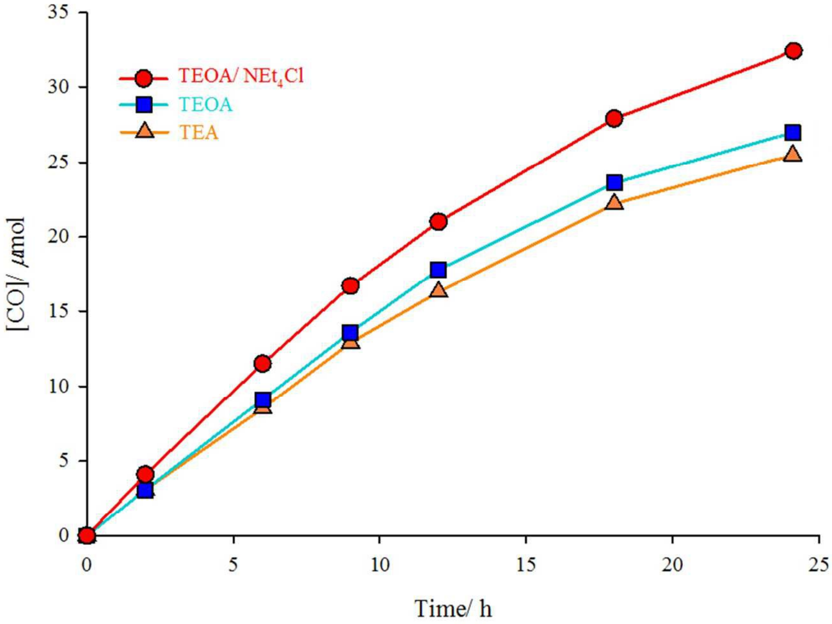

Fig. 3 Irradiation-time (h) dependence of the formation of CO (μmol) catalyzed by *fac*-[Re(phen-dione)(CO)$_3$Cl] under three different conditions: DMF/TEOA/ NEt$_4$Cl (red), DMF /TEOA (blue), and DMF/TEA (yellow).

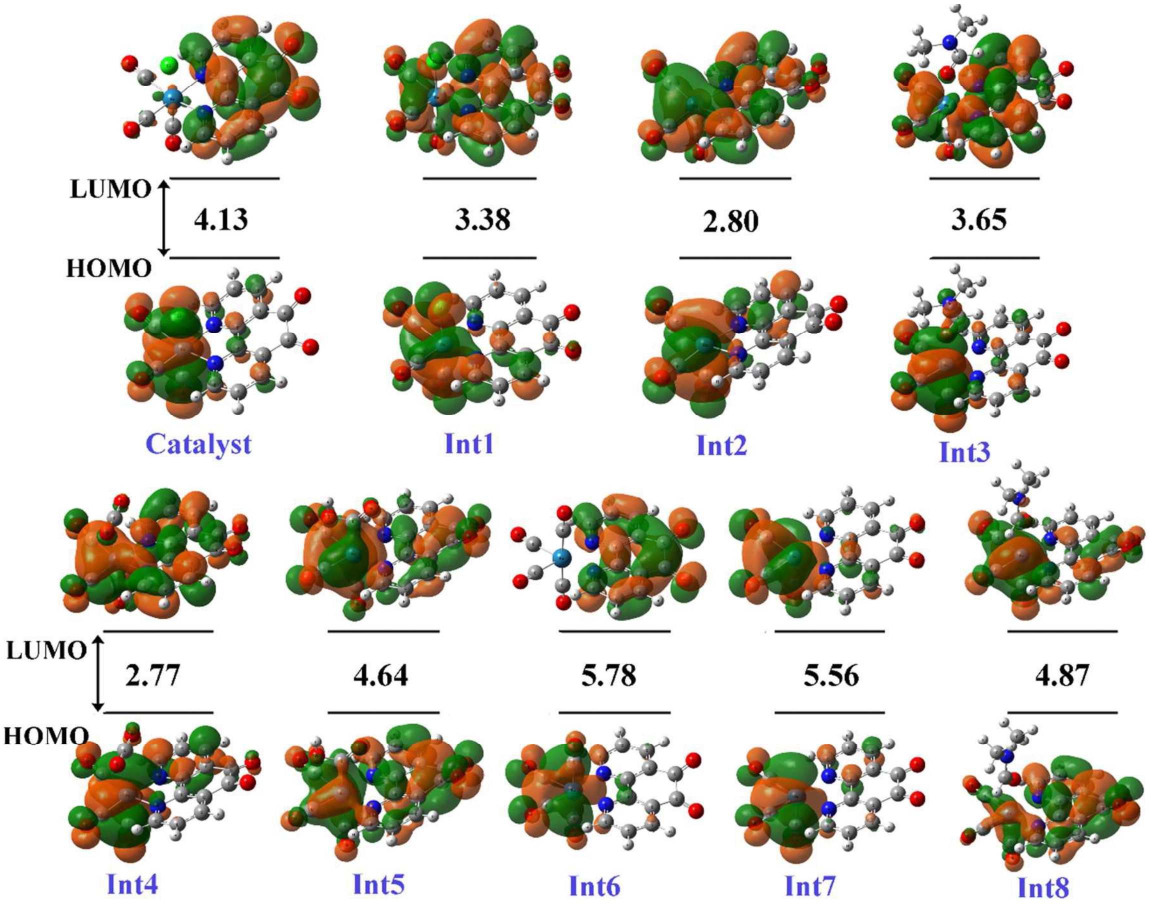

Fig. 4 The distribution and energy (eV) of FMOs (frontier molecular orbitals) of the species in the gas phase involved in the proposed mechanism.

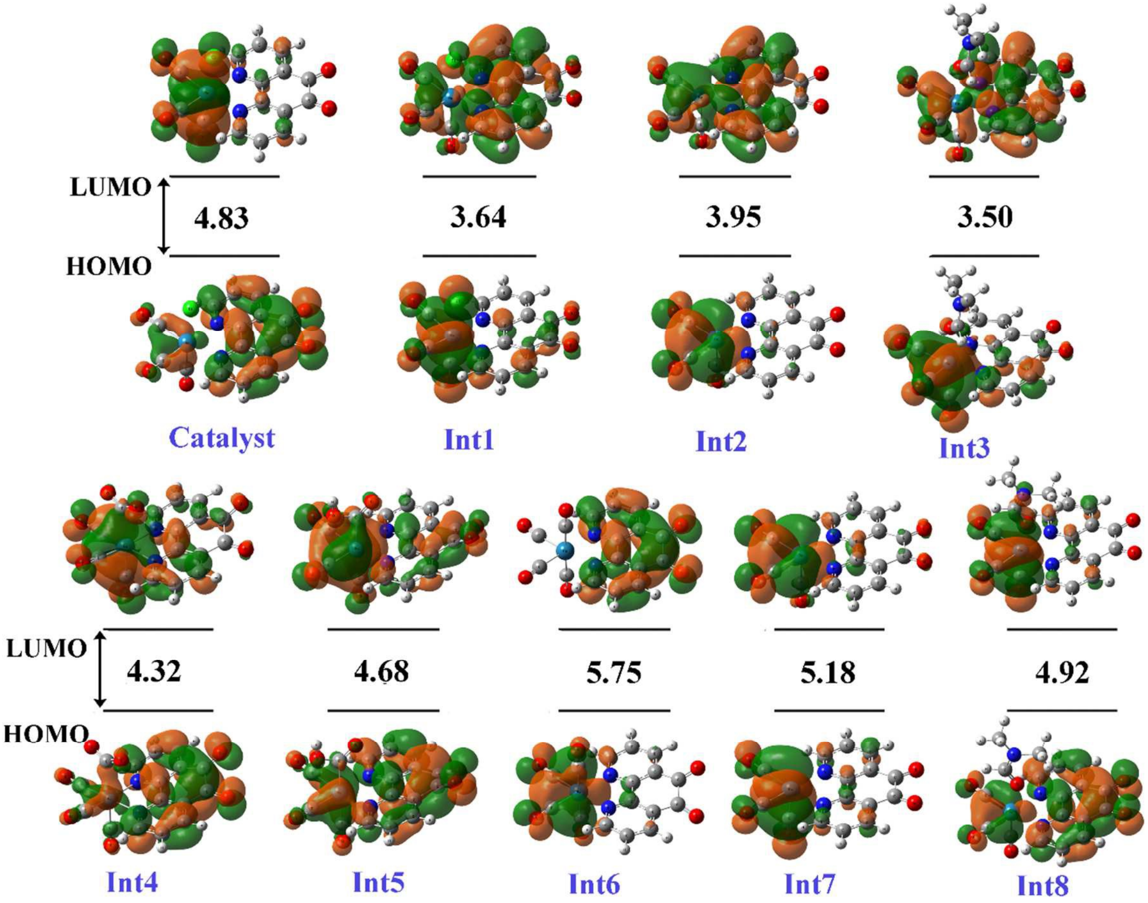

Fig. 5 The distribution and energy (eV) of FMOs of the species in the solution phase involved in the proposed mechanism.

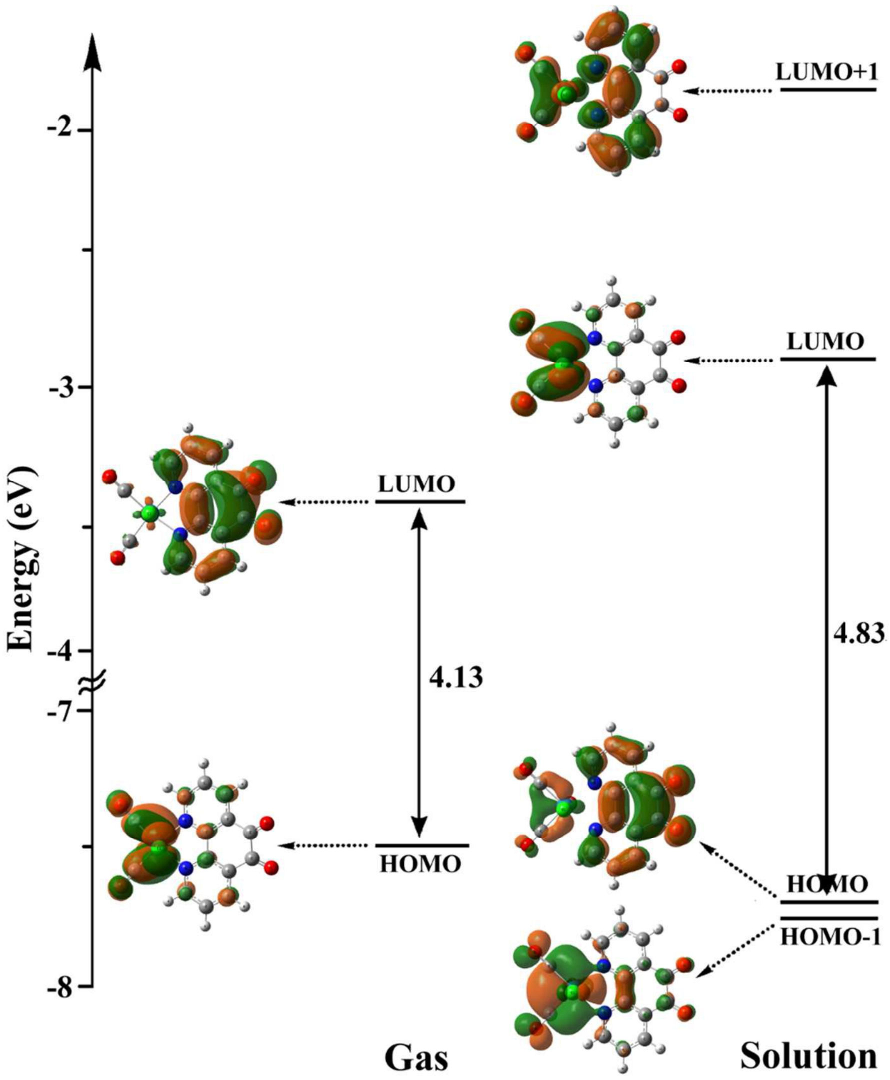

Fig. 6 The energy levels and shapes of HOMO - 1, HOMO, LUMO, and LUMO + 1 orbitals of the **Catalyst** in the gas phase and solution.